ICAIC International Conference for Academia and Industry Co-operation
09 a 13 de junho de 2025
Instituto Federal do Maranhão | Campus São Luís - Monte Castelo
5th IMMSEM International Meeting in Materials Science and Engineering of Maranhão

# CHARACTERIZATION OF MODIFIED SUPERMARTENSITIC STAINLESS STEELS GRADES

**Pedro S. P. Garcia[1*], Juan M. Pardal[2], Sérgio S. M. Tavares[2],**

*1 - Programa de Pós-graduação em Engenharia de Materiais - PPGEM, Universidade do Estado do Rio de Janeiro (UERJ), Rio de Janeiro, RJ, Brasil.*
*2 - Departamento de Engenharia Mecânica, Universidade Federal Fluminense (UFF), Niterói, Brasil.*
pedro.garcia@uerj.br

## ABSTRACT

*The current requirements of the oil and gas industry focus on the exploration of wells under increasingly severe operating conditions. In this context, the use of high corrosion resistance alloys is often crucial in process piping applications. These materials must also exhibit excellent mechanical properties to ensure durability and reliability. Among the recently studied alternatives, the modified supermartensitic stainless steel family exhibits the most favorable cost-effectiveness ratio, particularly in comparison to duplex stainless steels and nickel alloys. Various grades are produced using different alloying additions to benefit toughness, corrosion resistance, and mechanical strength. These can also result from processing techniques like double or triple tempering following hot rolling. In recent years, numerous studies have concentrated on titanium alloyed supermartensitic stainless steel, examining its mechanical properties and microstructural behavior under various processing methods. These investigations predominantly resulted in classifications of 80, 95, or 110 ksi grades. This study examines the mechanical and microstructural changes in supermartensitic stainless steels alloyed with vanadium and nitrogen, processed to meet the necessary mechanical properties, to verify their suitability in such applications. The nitrogen-alloyed material exhibited higher strength but showed increased susceptibility to embrittlement and variations in properties. In contrast, the vanadium-alloyed material demonstrated more stable and consistent results, despite having lower strength.*

**Keywords:** *Supermartensitic Stainless Steel; Microstructural characterization; Mechanical Properties; Heat Treatment.*

## INTRODUCTION

The Supermartensitic Stainless Steels (SMSS) alloy family represent a technological advancement over conventional martensitic stainless steels, such as the 13% chromium family, extensively used in Oil and Gas industry. The most basic SMSS features lower carbon content with additions of nickel and molybdenum (1,2). Other listed grades present additional microalloying elements such as nitrogen (Grade S41425), titanium (Grade S41426), and vanadium (Grade S41427). These are further categorized as 80, 95, and 110 ksi grades in ISO 13680 (3). Several previous studies have examined the influence of titanium addition in martensitic and supermartensitic stainless steels (4,5,6,2). The effects of vanadium additions in SMSS are focused on corrosion and stress corrosion resistance. An early study by Everson & Johnson (7) indicated that vanadium-modified UNS S41427 exhibited superior stress corrosion resistance when compared to other tested grades, including the titanium-modified UNS S41426. Additionally, research by Lee et. al. (8) suggested that vanadium carbides may serve as hydrogen trapping sites, thereby enhancing resistance to hydrogen embrittlement. However,

influence of vanadium in mechanical resistance and microstructural features of SMSS are still not thoroughly investigated. In the case of nitrogen, it is commonly employed as a partial substitution to carbon in solution hardening, but also increases pitting resistance and, as Krishna et. al. (9) pointed out, causes secondary hardening through fine chromium rich M2N nitride formation at about 500°C. Qi et. al. (10) later confirmed this statement; however, they pointed that excessive nitrogen additions might promote the formation of coarser chromium-rich M23C6 and Cr2N in the martensitic matrix. So, this work aims to better explore the mechanical and microstructural correlations of the UNS S41425 (N-alloyed) and the UNS S41427 (V-alloyed) grades, providing useful information in materials selection.

## MATERIALS AND METHODS

This study investigated two different compositions of supermartensitic stainless steels, as shown in Table 1. Both were received as hot-rolled pipes and followed the NACE MR0175 (11) recommendations for either double or single tempering. The nitrogen-modified UNS S41425 grade was solution-treated at 932°C for 6 hours, air-quenched, and then tempered at 620°C for 13 hours. The vanadium-modified UNS S41427 alloy was solution treated at 950°C for 6 hours, oil quenched, then double tempered at 620°C for 11 hours and 550°C for 7 hours with air cooling. Furthermore, all samples, except for the as-received (AR) ones, underwent solution treatment at 1000°C in an inert atmosphere furnace for one hour, followed by oil cooling. Subsequently, they were tempered for one hour at various selected temperatures. Additionally, considering the extensive process undertaken by the manufacturer to achieve reduced hardness, two alternative double tempering treatments have been proposed. The nomenclature for key test specimens are as follows: the first letter (N or V) stands for the nitrogen or vanadium modified grades; the second digit is related to the specimen condition (AR – as received; AQ – as quenched; QT – quenched and tempered; DT – quenched and double tempering); when applicable, the last number indicates the tempering temperature. So, the N-QT550 refers to the nitrogen modified alloy solution treated, quenched and tempered at 550°C for 1h. In the case of double tempering, the first proposition (DT1) was carried out at 670°C for 1h followed by a second tempering at 600°C for 2h. The DT2 consisted of tempering at 670°C for 1h followed by a second tempering at 600°C for 8h.

Table 1 – Material identification and chemical composition

| Id. | Chemical composition, wt. %, Fe balance | | | | | | | | | | | |
|---|---|---|---|---|---|---|---|---|---|---|---|---|
| | **C** | **Mn** | **Si** | **Cr** | **Ni** | **Mo** | **S** | **P** | **N** | **Ti** | **Nb** | **V** |
| **"N" Alloy** | 0.020 | 0.76 | 0.32 | 13.52 | 4.61 | 1.66 | 0.0002 | 0.02 | 0.07 | <0.01 | <0.01 | 0.03 |
| **"V" Alloy** | 0.016 | 0.35 | 0.20 | 12.16 | 5.40 | 1.95 | 0.0021 | 0.01 | 0.01 | <0.01 | - | 0.16 |

Microstructural characterization was carried out for each condition and consisted in Optical Microscopy (OM) and Scanning Electron Microscopy (SEM) equipped with Energy-Dispersive Spectroscopy (EDS) analysis and a Field Emission Gun (FEG) after etching with Villella's reagent. Complementary, magnetic measurements were performed to determine the retained austenite volume content ($\%\gamma_{rt}$), using a vibrating sample magnetometer (VSM) with maximum applied field of 1T, following the same methodology described in (12), where

austenite fraction was obtained by comparing the saturation magnetization of a 100% martensitic sample of the same composition with the saturation magnetization of a tempered sample. These results were compared to XRD measurements, where the austenite volume content was determined using a 45-130° angular length, step of 0.02° and counting time of 1s in a spinner sample holder. At all XRD tests, the applied voltage and current were of respectively 40kV and 40mA. Austenite quantification was carried out through Rietveld refinement method. Complementary EBSD images with phase quantification were made to identify reversed austenite in a selected condition. Mechanical characterization consisted in tensile tests using a cylindrical specimen with 4 mm gauge diameter as permitted by ASTM A370 (13). Vickers hardness was performed with 10 kgf load with 10 tests per condition. Charpy V-notch impact tests were carried out at -10°C with standard test coupon 10x10x55 $mm^3$ proposed by ASTM E23 (14). Tensile tests were made in duplicate, and Charpy impact tests were made in triplicate.

## RESULTS AND DISCUSSION

Fig. 1 presents the microstructure of selected test conditions to compare both compositions in terms of response to tempering. The samples N-AQ and V-AQ presented a typical lath martensite matrix, with sporadic presence of small inclusion particles such as manganese sulfide and silicon oxide, which were identified by semi quantitative composition analysis by EDS during SEM. It is possible to verify that the martensite packets are slightly bigger in the "N" alloy when compared to the vanadium modified sample. This trend changes after tempering at increasingly higher temperatures, where the "N" alloy presents a finer block and packet structure, as can be noted qualitatively when comparing the N-QT550 with V-QT550. It is also important to note that a higher number of precipitates are visible after tempering, mainly in the nitrogen alloyed samples. At higher temperatures the precipitates tend to form in packet, block and prior austenite grain boundaries, thus revealing these microstructural features more clearly.

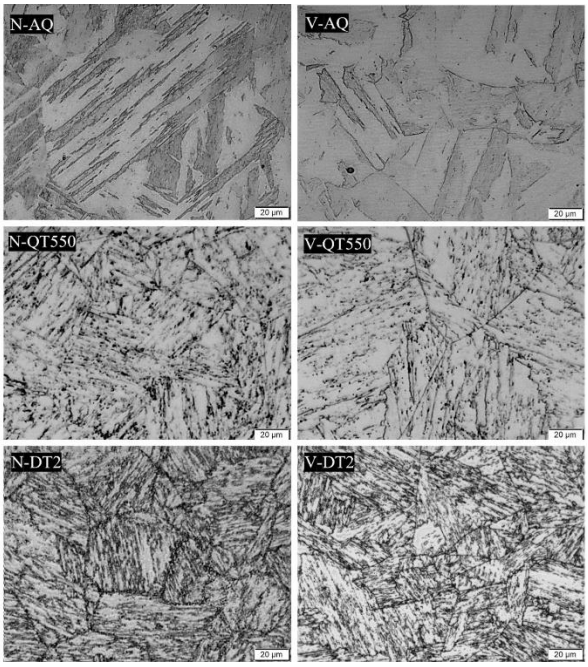

Fig. 1 – Optical micrography for both samples. Villela's reagent.

The SEM image presented in Fig. 2. presents further details of the sample's microstructure. Brighter features that appear near packet and block boundaries in the as quenched and tempered up to 550°C are richer in carbon, nickel and, in the case of "N" alloy, nitrogen. This figure indicates segregation in reverted austenite, as previously detected by Escobar et. al. (5,15), which increases gamma phase stability.

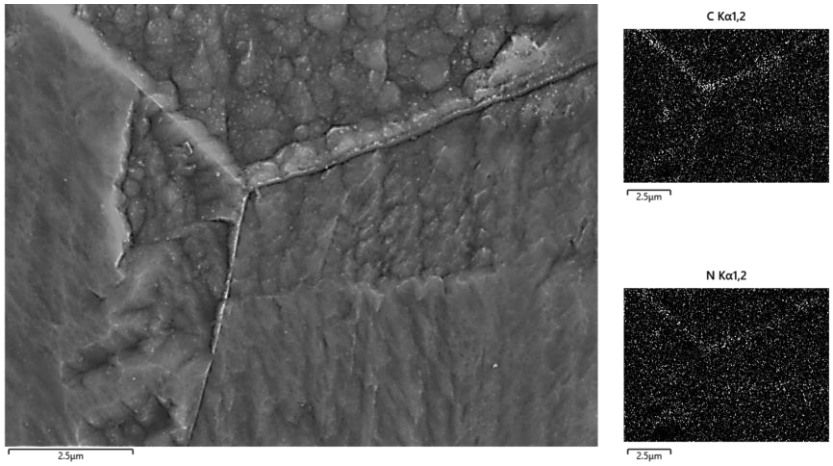


Fig. 2 – N-QT550 sample, SEM image with EDS map showing carbon and nitrogen segregation. Brighter areas present relatively higher element content.

The retained austenite fraction obtained by XRD and VSM measurements are presented in Table 2. It is important to state that XRD measurements are mainly superficial, with an extremely low penetration analysis, and the VSM is a more volumetric approach. That said, conventional metallographic preparation through sanding and etchant might interfere with the XRD $\gamma_{rt}$ quantification since the retained austenite is metastable and might undergo deformation induced transformation at the superficial layers. These factors have resulted in discrepancy when comparing both techniques. On the other hand, the saturation magnetization depends on the martensite composition, and since the tempering treatment leads to local nickel, carbon and nitrogen segregation in the samples, these results are also not perfectly accurate. It is, however, interesting to state that the difference between retained austenite fraction detected by both techniques indicates that γ phase in alloy V is more unstable, mainly in V-DT2 sample, since the volumetric analysis presented a considerably higher amount when comparing to the XRD analysis.

Table 2 – Retained austenite quantification.

| Id. | $\gamma_{rt}$ (XRD) | $\gamma_{rt}$ (VSM) | Id. | $\gamma_{rt}$ (XRD) | $\gamma_{rt}$ (VSM) |
|---|---|---|---|---|---|
| **N-AR** | 19.8 | 19.9 | **V-AR** | 17.5 | 25.3 |
| **N-AQ** | 0.0 | 2.0 | **V-AQ** | 0.0 | 0.8 |
| **N-QT500** | 0.0 | 1.5 | **V-QT500** | 0.0 | 0.1 |
| **N-QT550** | 0.0 | 0.0 | **V-QT550** | 0.0 | 0.8 |
| **N-QT650** | 3.6 | 6.9 | **V-QT650** | 0.0 | 7.3 |
| **N-DT1** | 17.4 | 18.1 | **V-DT1** | 18.0 | 13.9 |
| **N-DT2** | 14.9 | 17.9 | **V-DT2** | 5.7 | 20.3 |

Along with microstructural changes, tempering also greatly affects both alloy "N" and "V" mechanical properties, as can be seen in Fig. 3. Firstly, when compared to the "V" alloy,

the “N” alloy presented higher tensile strength, regardless of tempering temperature, as presented previously by Chales et. al. (16). However, with increased temperature, the difference in both material’s response to a similar heat treatment tends to minimize. The higher strength in N alloy is expected mainly due to solution strengthening by nitrogen and fine carbonitride formation during tempering, as reported by Ma et. al. (17). This effect is clearly more pronounced at 500°C. On the other hand, the V alloy depends mainly on the formation of vanadium, chromium, and molybdenum precipitates to harden, which takes a longer time and/or temperature to occur. As nitrogen and carbon are interstitial elements, they diffuse at higher rates than the substitutional nickel, chromium and vanadium, leading to faster reactions and responses to heating in the “N” alloy. Evaluating the ductility, both alloys are similar in terms of elongation, indicating that the homogeneous portion of strain, i.e., plastic region before necking, are similar in both materials. However, the “V” alloy presented a consistently higher area reduction for almost all tempering conditions, except near 500°C, where the values were very close at in both materials. This result indicates that the “V” alloy is indeed more ductile than the “N”.

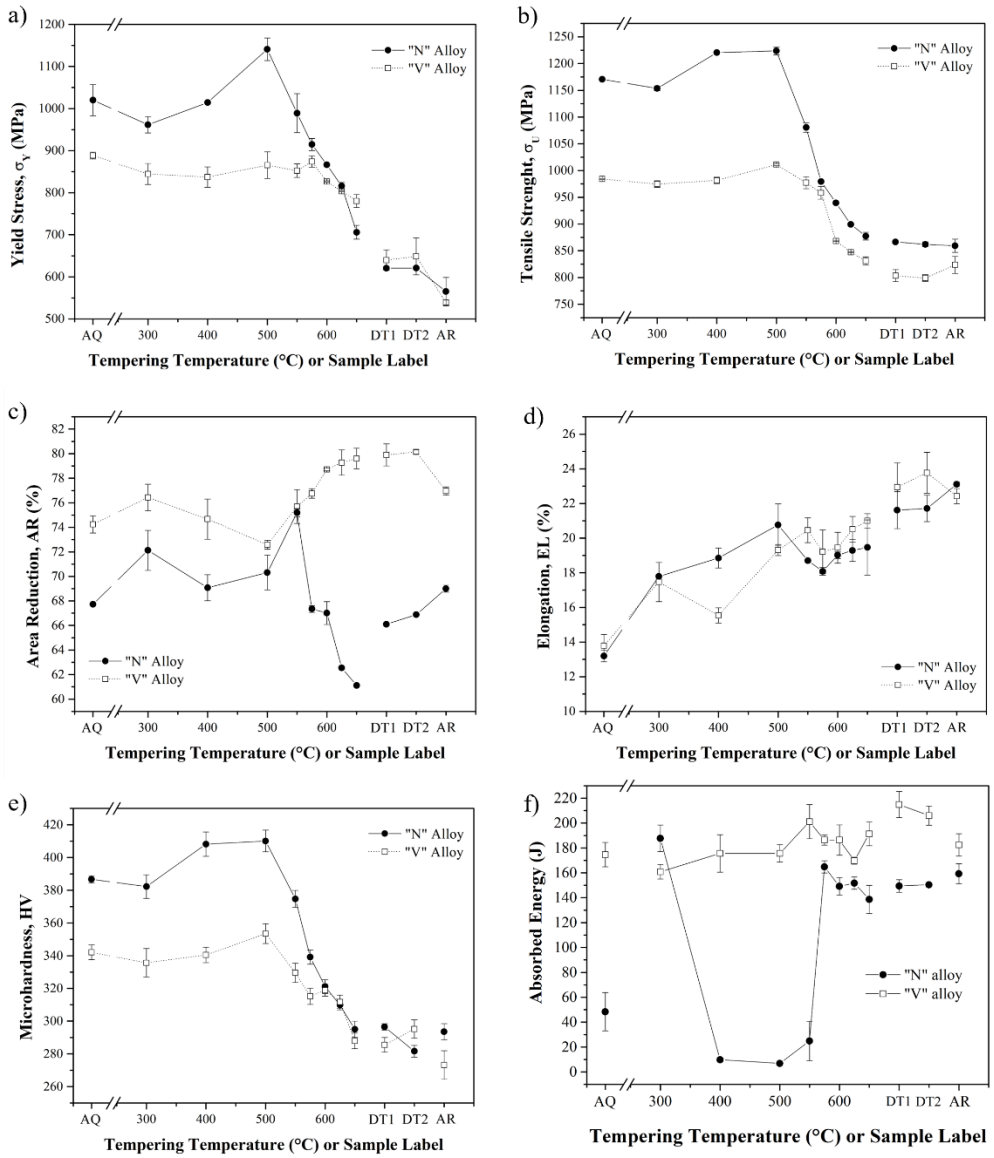


Fig. 3 – Mechanical properties of N and V alloys.

The presence of finely distributed precipitates along the martensitic matrix in the 550°C tempered samples, as can be seen in N-QT550 and V-QT550 at **Error! Reference source not found.** and Fig. 2 are one of the major hardening mechanisms responsible for higher tensile strength, hardness and comparatively lower toughness. These precipitates are mainly carbonitrides rich in chromium and molybdenum, as early works had pointed out (18,2). Fig. 3 (f) also points to a higher toughness in the vanadium alloyed sample. More importantly, there was no reduction in -10°C impact toughness accompanying the increase in strength as was the case in "N" alloy. Tempering above 600°C is recommended to avoid low toughness in the "N" alloy. The presence of coarser carbonitrides was already pointed out as the cause for both sensitization (19) and embrittlement. These different responses to mechanical tests are mainly due to carbonitride precipitation, which hardens the material but might also lead to toughness drop when coarsened.

## CONCLUSIONS

Comparing both studied alloys, the "N" alloyed sample presented higher variations in its mechanical properties, and, despite its higher strength and hardness, it is expected to present lower toughness in applications under 0°C. This temper embrittlement behaviour might be an issue in offshore industry, and a limiting factor in heat treatment and welding parameter selection. The vanadium alloy requires more time to present significant modifications in its mechanical properties, providing a more consistent and possibly repeatable result, possibly leading to better weldability and workability at several applications such as hot forming and rolling. The major hardening mechanism proposed for this steel family, is precipitation hardening, followed by solution strengthening. The nature of the microadditions used to achieve hardening will dictate the time and temperature required to achieve the best combination of results. Excessive tempering might lead to coarsening of precipitates in packets and block boundaries, and thus to embrittlement, as was evidenced for "N" alloy. Alloy "V", on the other hand, presents a more consistent result of impact toughness measured at -10ºC. There was no evidence of a direct correlation between the presence of retained austenite and an increase in toughness. However, it's highly probable that the presence of $\gamma_{rt}$ might have hindered the toughness drop due to precipitate coarsening in the higher tempering temperatures and double tempering treatments. Microhardness steep drop with increase of tempering temperature above 500°C corroborates the combination of both mechanisms: precipitate coarsening and increase in $\gamma_{rt}$, which were also confirmed by SEM images, XRD and Magnetic measurements, respectively.

## AKNOWLEDGEMENTS

This work was supported by Fundação Carlos Chagas Filho de Amparo à Pesquisa do Estado do Rio de Janeiro; Grant number E-26/210.877/2024 (295744);

## REFERENCES

[1] CALDERÓN-HERNÁNDEZ, J. W. et al. Electrochemical characterization of 13Cr low-carbon martensitic stainless steel - Corrosion study with a mini-cell setup. **Journal of Materials Research and Technology**, v. 21, p. 2989–2998, 1 nov. 2022.

[2] TAVARES, S. S. M. et al. Microstructure and Mechanical Properties of Ti-Alloyed Supermartensitic 12%Cr Stainless Steel Classes 95 ksi and 110 ksi for Oil and Gas

Production. **Journal of Materials Engineering and Performance**, v. 31, n. 10, p. 8004–8012, 1 out. 2022.
[3] ISO 13680. Petroleum and natural gas industries — Corrosion - resistant alloy seamless tubes for use as casing , tubing and coupling stock — Technical delivery conditions. 2010.
[4] RODRIGUES, C. A. D. et al. Effect of titanium nitride (TiN) on the corrosion behavior of a supermartensitic stainless steel. **Materials and Corrosion**, v. 70, n. 1, p. 28–36, 2019.
[5] ESCOBAR, J. D. et al. Meta-equilibrium transition microstructure for maximum austenite stability and minimum hardness in a Ti-stabilized supermartensitic stainless steel. **Materials and Design**, v. 156, p. 609–621, 2018.
[6] ESCOBAR, J. D. et al. Compositional analysis on the reverted austenite and tempered martensite in a Ti-stabilized supermartensitic stainless steel: Segregation, partitioning and carbide precipitation. **Materials and Design**, v. 140, p. 95–105, 2018.
[7] EVERSON, H.; JOHNSON, A. **Alloyed 13% Chromium Steel UNS S41427 For Completion Equipment And Tubing - Corrosion Tests In Simulated Well Fluids And Comparative Corrosion Test Data On Other 13%Cr Steels**. NACE Corrosion 2001. **Anais**...2001.
[8] LEE, J. et al. Effects of vanadium carbides on hydrogen embrittlement of tempered martensitic steel. **Metals and Materials International**, v. 22, n. 3, p. 364–372, 2016.
[9] KRISHNA, S. C. et al. Microstructure and Properties of Nitrogen-Alloyed Martensitic Stainless Steel. **Metallography, Microstructure, and Analysis**, v. 6, n. 5, p. 425–432, 2017.
[10] QI, X.; MAO, H.; YANG, Y. Corrosion behavior of nitrogen alloyed martensitic stainless steel in chloride containing solutions. **Corrosion Science**, v. 120, p. 90–98, 2017.
[11] NACE MR0175. Part 1 - Materials for use in H2S-containing environments in oil and gas production: General principles for selection of cracking-resistant materials. 2015.
[12] TAVARES, S. S. M. et al. Temper embrittlement of supermartensitic stainless steel and non-destructive inspection by magnetic Barkhausen noise. **Engineering Failure Analysis**, v. 100, p. 322–328, jun. 2019.
[13] ASTM A370. Standard Test Methods and Definitions for Mechanical Testing of Steel Products. **ASTM International**, 2022.
[14] ASTM E23. Standard Test Methods for Notched Bar Impact Testing of Metallic Materials. **ASTM International**, 2018.
[15] ESCOBAR, J. D. et al. Austenite reversion kinetics and stability during tempering of a Ti-stabilized supermartensitic stainless steel: Correlative in situ synchrotron x-ray diffraction and dilatometry. **Acta Materialia**, v. 138, p. 92–99, 2017.
[16] CHALES, R. et al. Mechanical Properties and Strain-Hardening Models of Supermartensitic Stainless Steels Alloyed to Nitrogen and Vanadium. **Materials Research**, v. 26, 2023.
[17] MA, X. et al. Studies on Nb microalloying of 13Cr super martensitic stainless steel. **Metallurgical and Materials Transactions A: Physical Metallurgy and Materials Science**, v. 43, n. 12, p. 4475–4486, 2012.
[18] DA SILVA, G. F. et al. Influence of heat treatments on toughness and sensitization of a Ti-alloyed supermartensitic stainless steel. **Journal of Materials Science**, v. 46, n. 24, p. 7737–7744, 2011.
[19] BAPTISTA, I. P. et al. Microstructure, mechanical properties, and corrosion resistance of supermartensitic steel UNS S41426: comparison between forged and hot-rolled

seamless pipe. **International Journal of Advanced Manufacturing Technology**, v. 123, n. 7–8, p. 2643–2653, 1 dez. 2022.